

Received May 19, 2022, accepted May 23, 2022, date of publication May 27, 2022, date of current version June 8, 2022.

Digital Object Identifier 10.1109/ACCESS.2022.3178602

# FDA-MIMO Radar Robust Beamforming Based on Matrix Weighting Method

CHANGLIN ZHOU<sup>1</sup>, CHUNYANG WANG<sup>1</sup>, JIAN GONG<sup>1</sup>, LEI BAO<sup>2</sup>,  
GENG CHEN<sup>1</sup>, AND MINGJIE LIU<sup>1</sup>

<sup>1</sup>Air and Missile Defense College, Air Force Engineering University, Xi'an 710051, China

<sup>2</sup>College of Information and Communication, National University of Defense Technology, Wuhan 430000, China

Corresponding author: Jian Gong (drgong@aliyun.com)

This work was supported by the Natural Science Foundation of Shanxi Province under Grants 2021JM-222.

**ABSTRACT** This paper deals with the problem of robust beamforming and target power estimation in the presence of main-lobe interference with frequency division array multiple-input multiple-output (FDA-MIMO) radar by adopting a weighting matrix at the receiving end. Based on the semi-definite programming (SDP) to solve the covariance matrix of the weighting matrix, we propose two beamforming methods and two methods for estimating the target power when the interference has a position error. Then, we propose obtaining the weighting matrix by performing singular value decomposition on the covariance matrix. We confirm the effectiveness of the developed method by comparing beam pattern and target signal estimation performance.

**INDEX TERMS** FDA-MIMO radar, semi-definite programming (SDP), weight matrix, beamforming, target power estimation.

## I. INTRODUCTION

The beamforming of phased array (PA) radar plays a vital role in interference suppression, which can focus energy in the direction of interest while suppressing signals in the interference direction [1]. The traditional beamforming method is to design complex-valued weight vectors to form the required beam pattern [2]. The idea of using SDP for beamforming based on amplitude least squares fitting was presented in [3]. When there are strong interferences, it is necessary to use an adaptive method to enhance the interference suppression capability [4], such as standard Capon beamformer (SCB), which adjusts the weight vector adaptively according to the input signal [5]. These traditional methods are vector weighting the signal to form a beam. However, literature [6] proposes an adaptive beamforming method using matrix weighting at the transmitting end, which is forming a group of beams first, and then beams are accumulated to a total beam. The algorithm proposed in [6] can only obtain the covariance matrix of the weighting matrix, and it does not give a method to obtain the weighting matrix. On this basis, literature [7] proposed a matrix-weighted robust beamforming method and has a better main lobe shape-preserving

The associate editor coordinating the review of this manuscript and approving it for publication was Cheng Hu<sup>1</sup>.

performance. At the same time, it can obtain the weighting matrix through orthogonal diagonal decomposition of the covariance matrix. However, obtaining the orthogonal matrix is still difficult. The papers mentioned above focus on phased arrays, which cannot effectively suppress range-dependent interferences through beamforming methods.

Since its proposal, FDA radar has attracted widespread attention in the research community [8], [9]. Different from the angle dependence of the PA radar beam, the beam of the FDA radar is range-angle-time depending by introducing a small frequency increment between the array elements [10]. On one hand, the FDA radar beam pattern is range-dependent, it may be beneficial to suppress range-dependent interference [11]. On the other hand, the beam pattern of FDA radar has time-varying characteristics, which will increase the complexity of radar system interface processing [12]. The literature [13] further pointed out that FDA radar cannot form a range-dependent and time-independent transmit beam pattern. It is necessary to adopt correct signal processing methods at the receiving end to activate the range-dependent of the FDA radar. Therefore, multiple-input multiple-output (MIMO) technology is suggested to combine with FDA radar [14].

The beam pattern design of FDA-MIMO radar mainly focuses on two aspects: frequency increment and

weight vector. Frequency increment design mainly focuses on heuristic methods, such as non-linear frequency offset design or multiple carrier frequency designs, lacking specific optimization design criteria [15]–[17]. Based on minimizing the area of the main lobe as the criterion, [18] obtained the analytical solution of the frequency increment. Using genetic algorithm and particle swarm optimization algorithm, literature [19], [20] obtains the frequency increment to make the beam sidelobe energy lowest. It can be seen that the development trend of frequency increment design from heuristic algorithm to optimal strategy. In addition to forming an ideal FDA-MIMO radar beam pattern through frequency increment design, weight vector optimization is another method of FDA-MIMO radar beamforming. By designing the weight vector, the beamforming problem can be transformed into a convex optimization problem with specific optimization criteria to make beamforming more flexible, such as flat-top beamforming [21] and sidelobe level reduction [22], [23]. However, the performance of the beam pattern will be significantly degraded when there are range-depend interferences and array steering vector errors. Reference [24] achieved the tracking of moving targets by jointly optimizing the transmitting weight vector and the receiving weight vector. Reference [25] developed to form a transceive beam pattern with broadened and deep nulls in the FDA-MIMO radar by optimizing the weight vector, then applied to imaging to overcome the interference problem. Reference [26] achieves high-resolution estimation of range and angle by optimizing the transmit beam space.

Inspired by the literature [6] that the matrix weighting of the signal at the transmitting improves degrees of freedom (DOF) of the system and the beam robustness, in this paper, we propose a robust beamforming method that performs matrix weighting on the FDA-MIMO radar received signals after multi-match filtering. We considered two beamforming methods and two target power estimation methods. For all methods, we obtain the covariance matrix of the weighting matrix through SDR, which is also the globally optimal solution to the problems. Then, we propose a method to obtain the weighted matrix through matrix singular value decomposition. Finally, the new weighting matrix is constructed by selecting the eigenvectors corresponding to the large eigenvalues, which reduces the complexity of the systems. At the analysis stage, the superiority of the proposed methods is verified by comparison with other classical beamforming methods.

The rest of the paper is organized as follows. In Section II, we derive a matrix-weighted FDA-MIMO radar receiving signal model. In Section III, two matrix-weighted beamforming methods are proposed to suppress potential or explicit interference signals. Then, we propose two target power estimation methods when there is an error in the interference position. In Section IV, We deduced the method of obtaining the weighting matrix through the singular value decomposition of the matrix. In Section V, We provide some simulations to verify the proposed robust

beamforming methods. Finally, concluding summaries are drawn in Section VI.

*Notation:* We use boldface for vectors  $\mathbf{a}$  and matrices  $\mathbf{A}$ . Scalar  $a$  is denoted by italicized. The transpose and conjugate transpose are denoted by the symbols  $(\cdot)^T$  and  $(\cdot)^H$  respectively.  $\mathbf{I}_M$  is  $M \times M$ -dimensional identity matrix.  $\otimes$  denotes the Kronecker product.  $\|\mathbf{a}\|$  and  $\text{trace}(\mathbf{A})$  present the two-norm of  $\mathbf{a}$  and the trace of matrix  $\mathbf{A}$ , respectively. The letter  $j$  represents the imaginary unit (i.e.  $j = \sqrt{-1}$ ).

## II. SIGNAL MODEL OF FDA-MIMO RADAR

We consider a narrow-band FDA-MIMO radar system including  $N_t$  transmitting elements and  $N_r$  receiving elements. Both the receiving array and the transmitting array are uniform linear arrays (ULA). To separate the FDA-MIMO radar transmission waveform and activate the range-dependent of its beam pattern at the receiving end, consider the received signal processing scheme proposed in [27], [28]. After multiple matched filtering, the received signal can be expressed as:

$$\mathbf{y}(r, \theta) = \alpha_0 \mathbf{a}_r(\theta_0) \otimes \mathbf{a}_t(r_0, \theta_0) + \sum_{j=1}^Q \alpha_j \mathbf{a}_r(\theta_j) \otimes \mathbf{a}_t(r_j, \theta_j) + \mathbf{n} \quad (1)$$

$$\mathbf{a}_r(\theta) = [1, \dots, e^{j2\pi f_0(N_r-1)d_R \sin \theta/c}]^T \quad (2)$$

$$\mathbf{a}_t(r, \theta) = [1, \dots, e^{j2\pi[-f(N_t-1)2r/c + f_0(N_t-1)d_T \sin \theta/c]}]^T \quad (3)$$

where,  $\mathbf{a}_r(\theta)$  and  $\mathbf{a}_t(r, \theta)$  represent the receiving and transmitting steering vectors, respectively.  $\alpha_0$  and  $\alpha_j$  represent the strength of the received target and interference signals, which is related to RCS and path attenuation. The target is located at  $(r_0, \theta_0)$ , and the interferences are located at  $(r_j, \theta_j)$ ,  $j = 1, \dots, Q$ .  $Q$  represents the number of interference sources. Without loss of generality, we assume that  $\mathbf{n}$  is the white Gaussian noise vector with zero mean and variance  $\sigma_n^2 \mathbf{I}_{N_t N_r}$ .  $f_0$  is the carrier frequency of the transmit signal, and  $f(N_t - 1)$  is the frequency increment of the  $N_t$ -th transmitting array element.

To improve the DOF of the radar system, we use a matrix  $\mathbf{W}$  instead of a vector to weigh the received signal after multiple matched filtering. After the received signal is weighted, it can be written as:

$$\mathbf{x}(r, \theta) = \mathbf{W}^H \mathbf{y}(r, \theta) \quad (4)$$

$$\mathbf{W} = [\mathbf{w}_1, \mathbf{w}_2, \dots, \mathbf{w}_M] \in C^{N_t N_r \times M} \quad (5)$$

To maximize the receiving beam pattern of the FDA-MIMO radar at the target, we assume:

$$\left\| \mathbf{W}^H \mathbf{a}_r(\theta_0) \otimes \mathbf{a}_t(r_0, \theta_0) \right\|^2 = 1 \quad (6)$$

We assume that  $\left\| \mathbf{W}^H \left( \sum_{j=1}^Q \alpha_j \mathbf{a}_r(\theta_j) \otimes \mathbf{a}_t(r_j, \theta_j) + \mathbf{n} \right) \right\|^2 \rightarrow 0$ , that is, the matrix-weighted beamforming method has a good suppression effect on interference and noise. As a result, we can further realize the estimation of the target signal power,

which can be expressed as:

$$\rho = \left\| \mathbf{W}^H \mathbf{y}(r, \theta) \right\|^2 = \left\| \alpha_0 \mathbf{W}^H \mathbf{a}_r(\theta_0) \otimes \mathbf{a}_r(r_0, \theta_0) \right\|^2 = \|\alpha_0\|^2 \quad (7)$$

The target power can be estimated without distortion when there is no interference by using the non-adaptive beamforming (NAB) method ( $w = \mathbf{a}_r(\theta_0) \otimes \mathbf{a}_r(r_0, \theta_0)$ ). However, it will inevitably bring about an error in the target power estimation when adjusting the weight vector to suppress interference. The method of matrix weighting the received signal proposed in this paper is a good trade-off between interference suppression and power estimation.

After being weighted by the matrix  $\mathbf{W}$ , the beam energy is focused on the target while effectively suppressing interferences and noise. Let  $\mathbf{a}(r, \theta) = \mathbf{a}_r(r, \theta) \otimes \mathbf{a}_t(r, \theta)$ . The problem  $\Gamma$  of obtaining the  $\mathbf{W}$  can be described as:

$$\Gamma : \min_{\mathbf{W}} \left\| \mathbf{W}^H \left( \sum_{j=1}^Q \alpha_j \mathbf{a}(r_j, \theta_j) + \mathbf{n} \right) \right\|^2$$

$$s.t. \quad \left\| \mathbf{W}^H \mathbf{a}(r_0, \theta_0) \right\|^2 = 1 \quad (8)$$

Applying (9), (8) can be rewritten as:

$$\left\| \mathbf{A}^H \mathbf{b} \right\|^2 = \left\| \mathbf{b}^H \mathbf{A} \right\|^2 = \mathbf{b}^H \mathbf{A} \mathbf{A}^H \mathbf{b} = \text{trace}(\mathbf{b}^H \mathbf{A} \mathbf{A}^H \mathbf{b})$$

$$= \text{trace}(\mathbf{A} \mathbf{A}^H \mathbf{b} \mathbf{b}^H) \quad (9)$$

$$\Gamma' : \min_{\mathbf{T}} \text{trace}(\mathbf{T} (\sum_{j=1}^Q \beta_j \mathbf{A}(r_j, \theta_j) + \sigma_n^2 \mathbf{I}_{N_t N_r}))$$

$$s.t. \quad \text{trace}(\mathbf{T} \mathbf{A}(r_0, \theta_0)) = 1$$

$$\text{trace}(\mathbf{T}) \geq \Gamma$$

$$\mathbf{T} \geq 0 \quad (10)$$

where,  $\mathbf{T} = \mathbf{W} \mathbf{W}^H$  and  $\mathbf{A}(r, \theta) = \mathbf{a}(r, \theta) \mathbf{a}^H(r, \theta)$  are Hermite matrix, respectively.  $\Gamma > 0$  is a small value introduced to prevent the optimization result from being zero.  $\beta_j = \alpha_j^2$  represents the energy of interference. The time complexity of the quasi-convex optimization problem is mainly related to the dimension of its optimization parameters, and the time complexity of  $\Gamma'$  is  $O(N_r^{3.5} N_t^{3.5})$ . The optimization methods proposed in the following papers are still a quasi-convex optimization problem, and their time complexity is also  $O(N_r^{3.5} N_t^{3.5})$ . Consequently, transmit-receive beam pattern is given by:

$$\mathbf{P}(r, \theta) = \left\| \mathbf{W}^H \mathbf{a}(r, \theta) \right\|^2 \quad (11)$$

### III. PROPOSED APPROACH

In this section, we propose a beam pattern matching method for suppressing potential interfering signals and a beamforming method for suppressing deterministic interfering signals. Then, we propose two robust beamforming methods to suppress interfering signals with position errors.

#### A. BEAM PATTERN MATCHING FOR MATRIX METHOD

We first consider a simple case of beam pattern matching, in which we know the location of the target and there may be main lobe interferences at some ranges. We can optimize  $\mathbf{T}$  so that the beam energy in the area will be below the set value, where there may be main lobe interferences. The problem  $\Gamma'$  can be rewrite as:

$$\Gamma'_1 : \min_{\mathbf{T}} \text{trace}(\sigma_n^2 \mathbf{T} \mathbf{I}_{N_t N_r})$$

$$s.t. \quad \text{trace}(\mathbf{T} \mathbf{A}(r_0, \theta_0)) = 1$$

$$\text{trace}(\mathbf{T} \mathbf{A}(r_l, \theta_0)) \leq \tau$$

$$\text{trace}(\mathbf{T} \mathbf{A}(r_m, \theta_0)) \leq u$$

$$\text{trace}(\mathbf{T} \mathbf{A}(r_m, \theta_0)) \geq l$$

$$\text{trace}(\mathbf{T}) \geq \Gamma$$

$$\mathbf{T} \geq 0 \quad (12)$$

where,  $r_l \in \psi_l$  and  $r_m \in \psi_m$  are the range where interferences and target may exist respectively.  $\tau$ ,  $u$  and  $l$  are the set energy threshold. The objective function of optimization is to minimize noise, which is a real map. The increase of constraints is to make the energy of a paragraph range within the main lobe lower or higher than the set threshold.  $\Gamma'_1$  is an SDP problem that can be efficiently solved by MTTLAB's CVX toolbox [29], [30].

#### B. ADAPTIVE BEAMFORMING FOR MATRIX METHOD

Next, we consider another case of main lobe interference where the positions of the interference and the target are known. The optimized objective function is to minimize the energy of interference and noise while the gain of the beam pattern at the target is one. We cannot solve optimization problem  $\Gamma'$  using the CVX toolbox because its objective function is not a real map. We need to reformulate the optimization problem  $\Gamma'$ . The interference and noise power can be expressed as:

$$\mathbf{Y}_{j+n} = \sum_{j=1}^Q \beta_j \mathbf{A}(r_j, \theta_j) + \sigma_n^2 \mathbf{I}_{N_t N_r} \quad (13)$$

$\mathbf{Y}_{j+n}$ ,  $\mathbf{A}(r_0, \theta_0)$  and  $\mathbf{T}$  can be transformed into the real domain and expressed as [31]:

$$\widetilde{\mathbf{Y}}_{j+n} = \begin{bmatrix} \Re(\mathbf{Y}_{j+n}) & -\Im(\mathbf{Y}_{j+n}) \\ \Im(\mathbf{Y}_{j+n}) & \Re(\mathbf{Y}_{j+n}) \end{bmatrix} \in \mathbb{R}^{2N_t N_r \times 2N_t N_r} \quad (14)$$

$$\widetilde{\mathbf{A}}(r_0, \theta_0) = \begin{bmatrix} \Re(\mathbf{A}(r_0, \theta_0)) & -\Im(\mathbf{A}(r_0, \theta_0)) \\ \Im(\mathbf{A}(r_0, \theta_0)) & \Re(\mathbf{A}(r_0, \theta_0)) \end{bmatrix} \in \mathbb{R}^{2N_t N_r \times 2N_t N_r} \quad (15)$$

$$\widetilde{\mathbf{T}} = \begin{bmatrix} \Re(\mathbf{T}) & -\Im(\mathbf{T}) \\ \Im(\mathbf{T}) & \Re(\mathbf{T}) \end{bmatrix} \in \mathbb{R}^{2N_t N_r \times 2N_t N_r} \quad (16)$$

$\Gamma'$  can be reformulated in the real domain as:

$$\Gamma'_2 : \min_{\widetilde{\mathbf{T}}} \text{trace}(\widetilde{\mathbf{T}} \widetilde{\mathbf{Y}}_{j+n})$$

$$s.t. \quad \text{trace}(\widetilde{\mathbf{T}} \widetilde{\mathbf{A}}(r_0, \theta_0)) = 1$$

$$\text{trace}(\widetilde{\mathbf{T}}) \geq \Gamma$$

$$\widetilde{\mathbf{T}} \geq 0 \quad (17)$$

Finally, we can extract the covariance matrix of the weighting matrix  $\mathbf{T}$  from  $\tilde{\mathbf{T}}$  as:

$$\mathbf{T} = \tilde{\mathbf{T}}(1 : N_t N_r, 1 : N_t N_r) + j\tilde{\mathbf{T}}(N_t N_r + 1 : 2N_t N_r, 1 : N_t N_r) \quad (18)$$

### C. POWER ESTIMATION

We evaluate the effectiveness of the interference suppression method by the accuracy of the target power estimation. The adaptive beamforming method proposed above is sensitive to the steering vector. When there is an error in the interference position, the interference suppression method may fail. Therefore, we first propose widening the main lobe interference null.

#### 1) MAIN LOBE NULL WIDENING METHOD

We obtain the main lobe interference range as  $r_j$  by prior information. Assuming that the error between the interference range obtained by prior information and the real interference range is within  $\Delta$ , we set the null width of  $2\Delta$  with  $r_j$  as the center. Then, the new interference and noise power can be rewrite as:

$$\mathbf{Y}'_{j+n} = \sum_{j=1}^Q \beta_j \mathbf{A}(\tilde{r}_j, \theta_j) + \sigma_n^2 \mathbf{I}_{N_t N_r} \quad (19)$$

where,  $\tilde{r}_j \in [r_j - \Delta, r_j + \Delta]$ ,  $\mathbf{Y}'_{j+n}$  is transformed into the real-domain form  $\tilde{\mathbf{Y}}'_{j+n}$ , and the optimization problem  $\Gamma'_2$  can be reformulated as:

$$\begin{aligned} \Gamma''_2 : \quad & \min_{\tilde{\mathbf{T}}} \text{trace}(\tilde{\mathbf{T}}\tilde{\mathbf{Y}}'_{j+n}) \\ & \text{s.t. } \text{trace}(\tilde{\mathbf{T}}\tilde{\mathbf{A}}(r_0, \theta_0)) = 1 \\ & \text{trace}(\tilde{\mathbf{T}}) \geq \Gamma \\ & \tilde{\mathbf{T}} \geq 0 \end{aligned} \quad (20)$$

In optimization problem  $\Gamma''_2$ , the interferences are suppressed by widening the null. However, through simulation experiments, we found another phenomenon that the radar beam pattern cannot achieve the maximum value at the target, resulting in errors in the estimation of the target power. We try to find a method that can take into account both robust interference suppression and target power estimation.

#### 2) LOW POWER BEAM MATCHING METHOD

When we minimize the energy of interference, a phenomenon occurs where the energy in other locations will increase. In fact, we do not need to minimize the interference signal but only need to reduce the interference energy to a suitable value so that it does not affect the detection of the target signal. Therefore, we propose a beam-matching method to achieve robust interference suppression. The signal power of the interference source can be roughly obtained by the method mentioned above or the SCB. We can set the threshold  $\tau$  for beam matching based on the estimated interfering signal

power. The optimization problem  $\Gamma'_1$  can be reformulated as:

$$\begin{aligned} \Gamma''_1 : \quad & \min_{\mathbf{T}} \text{trace}(\sigma_n^2 \mathbf{T}\mathbf{I}_{N_t N_r}) \\ & \text{s.t. } \text{trace}(\mathbf{T}\mathbf{A}(r_0, \theta_0)) = 1 \\ & \text{trace}(\mathbf{T}\mathbf{A}(\tilde{r}_j, \theta_0)) \leq \tau \\ & \text{trace}(\mathbf{T}) \geq \Gamma \\ & \mathbf{T} \geq 0 \end{aligned} \quad (21)$$

The optimization problem  $\Gamma''_1$  can be efficiently solved by the CVX toolbox. The optimization problem optimizes the covariance matrix  $\mathbf{T}$  of the weighting matrix, not the weighting matrix  $\mathbf{W}$ , so we also need to solve a vital problem to use  $\mathbf{T}$  to obtain  $\mathbf{W}$ .

### IV. SINGULAR VALUE DECOMPOSITION METHOD TO FIND WEIGHTING MATRIX

[6] first proposed a beamforming method of matrix weighting the transmitted signal and obtained the covariance matrix of the weighting matrix  $\mathbf{T}$  by the optimization problem, but failed to determine the weighting matrix  $\mathbf{W}$ . Further, [7] proposed a method to obtain  $\mathbf{W}$  by performing orthogonal diagonal decomposition of  $\mathbf{T}$ , which provides a vital idea. However, it does not explain how to determine the orthogonal matrix simply and efficiently, so further exploration is required. We consider using the singular value decomposition method of the matrix because the required unitary matrix and singular values can be effectively obtained by the function ‘svd’ of MATLAB.

$\mathbf{T} = \mathbf{W}\mathbf{W}^H$  is the Hermite matrix whose eigenvalues are positive real numbers and can be expressed as:

$$\lambda_1 \geq \lambda_2 \geq \dots \geq \lambda_r > \lambda_{r+1} = \dots = \lambda_{N_t N_r} = 0 \quad (22)$$

$\sigma_i = \sqrt{\lambda_i}$  ( $i = 1, 2, \dots, N_t N_r$ ) is the singular value of  $\mathbf{W}$ .  $r = \text{rank}(\mathbf{W})$  is equal to the number of non-zero singular values of  $\mathbf{W}$ . Performing singular value decomposition on  $\mathbf{W}$  can be expressed as:

$$\mathbf{W} = \mathbf{U} \begin{bmatrix} \boldsymbol{\Sigma} & \mathbf{0} \\ \mathbf{0} & \mathbf{0} \end{bmatrix} \mathbf{V}^H \quad (23)$$

where,  $\boldsymbol{\Sigma} = \text{diag}(\sigma_1, \sigma_2, \dots, \sigma_r)$ .  $\mathbf{U} \in \mathbb{C}^{N_t N_r \times N_t N_r}$  and  $\mathbf{V} \in \mathbb{C}^{M \times M}$  are unitary matrix. Introducing (23),  $\mathbf{T}$  can be further expressed as:

$$\begin{aligned} \mathbf{T} = \mathbf{W}\mathbf{W}^H &= \mathbf{U} \begin{bmatrix} \boldsymbol{\Sigma}^2 & \mathbf{0} \\ \mathbf{0} & \mathbf{0} \end{bmatrix} \mathbf{U}^H = \mathbf{U} \begin{bmatrix} \boldsymbol{\Sigma}^2 & \mathbf{0} \\ \mathbf{0} & \mathbf{0} \end{bmatrix} \mathbf{V}_T^H \\ &= \mathbf{U} \begin{bmatrix} \boldsymbol{\Sigma} & \mathbf{0} \\ \mathbf{0} & \mathbf{0} \end{bmatrix} \left( \begin{bmatrix} \boldsymbol{\Sigma} & \mathbf{0} \\ \mathbf{0} & \mathbf{0} \end{bmatrix} \mathbf{U} \right)^H \end{aligned} \quad (24)$$

where,  $\mathbf{V}_T = \mathbf{U}$  and  $\mathbf{U}$  are unitary matrices obtained by performing singular value decomposition of  $\mathbf{T}$ , and  $\boldsymbol{\Sigma}^2$  is the singular value of  $\mathbf{T}$ .  $\mathbf{W}$  can be rewritten as:

$$\mathbf{W} = \mathbf{U} \begin{bmatrix} \boldsymbol{\Sigma} & \mathbf{0} \\ \mathbf{0} & \mathbf{0} \end{bmatrix} \quad (25)$$

By observing (25), we can find that the singular values of  $\mathbf{W}$  may contain zero and small real numbers that have little



influence on the receiving beam that can ignore to reduce the dimension of  $\mathbf{W}$ . We select  $P$  singular values whose criteria are as follow:

$$\sigma_P \geq \sigma_1/\eta > \sigma_{P+1} \tag{26}$$

Let  $\Sigma' = \text{diag}(\sigma_1, \sigma_2, \dots, \sigma_P)$ .  $\mathbf{U}' \in \mathbb{C}^{M_t N_r \times P}$  is a matrix composed of vectors represented by the selected eigenvalues.  $\eta$  is an empirical value representing the criterion for selecting singular values. Finally, the weighting matrix  $\mathbf{W}$  can be expressed as:

$$\mathbf{W}' = \mathbf{U}' \Sigma' \tag{27}$$

More importantly, traditional vector weighting methods are not convex, and convexity can only be satisfied by dropping the rank-one constraint. However, the matrix weighting method is convex and can be solved efficiently by the CVX toolbox, so we consider that the matrix weighting method has better performance.

### V. SIMULATION RESULTS

In simulations, we consider an FDA-MIMO radar consisting of 10 transmit elements and 10 receive elements with a half wavelength inter-element spacing. The frequency offset is set to  $5\text{kHz}$ , weighted by a non-uniform coefficient of the Hamming window [17]. The target is located at  $(20\text{km}, 30^\circ)$ , and its signal-to-noise ratio (SNR) is  $20\text{dB}$  and the speed of light is  $c = 3 \times 10^8\text{m/s}$ . Without loss of generality, we choose  $\Gamma = 0.001$ ,  $\eta = 100$ ,  $\tau = -50\text{dB}$ ,  $u = 0\text{dB}$  and  $l = -0.5\text{dB}$ . These simulation parameters will not be changed unless otherwise specified. In the range-angle beam pattern measured in decibels, data below  $-50\text{dB}$  is approximated to  $-50\text{dB}$  to improve beam pattern comparison.

*Example 1:* In this example, we first verify the beam pattern matching for matrix (BPMM) method performance and then compare its performance with the NAB method in the range dimension. We set the area where there may be interference as  $r_l \in [40\text{km}, 50\text{km}]$  and where there may be targets as  $r_m \in [19.5\text{km}, 20.5\text{km}]$  and  $\theta_m \in [29^\circ, 31^\circ]$ . Fig.1 shows the beam pattern performance using the BPMM method and the NAB method, respectively.

Fig.1 shows that NAB does not have the potential for main lobe anti-jamming, while BPMM has good beam matching performance and can suppress potential main lobe interference. The comparison of the gain in the range dimension and the spatial energy focusing of the two methods is shown in Fig.2.

We can see from Fig.2 that BPMM can bring the beam gain below the set threshold in areas where there may be interference. Although BPMM causes a small main lobe expansion compared to NAB, it brings a good interference suppression potential.

*Example 2:* In this example, we perform adaptive beamforming for matrix (ABM) method by substituting  $\mathbf{W}'$  for the weighting vector in SCB. Furthermore, we compare the performance of ABM, NAB, and SCB methods for interference suppression. It is assumed that there are

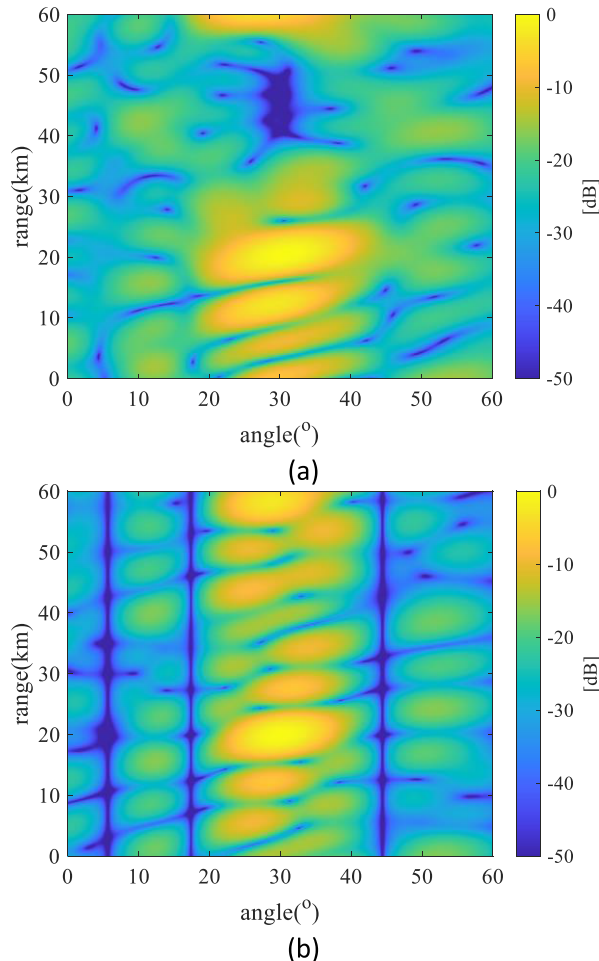


FIGURE 1. Comparison of range-angle beam patterns for (a) BPMM and (b) NAB.

three signal-dependent interferences located at  $(30\text{km}, 30^\circ)$ ,  $(40\text{km}, 30^\circ)$ , and  $(50\text{km}, 30^\circ)$ . The interference-to-noise ratio (INR) is  $40\text{dB}$ . Fig.3 shows the comparison of beam pattern in the range dimension.

It is noted from Fig.3 that both ABM and SCB can effectively suppress main lobe interference. The nulls of SCB at the interference place are greater than that of ABM, which is caused by the rejection of small eigenvalues by ABM. It can be seen that the performance of ABM is inferior to that of SCB when the interference position is known (the steering vector is accurate). However, when there is an interference position error, the performance of ABM will be better than that of SCB because it increases DOF of the systems and brings about the improvement of robustness.

*Example 3:* In this example, We consider comparing the robustness of the main lobe null widening (MNW) method, low power beam matching (LPBM) method, SCB, and NAB by beam pattern and target power estimation. The interference location and INR is the same as example 2, but it includes the range error  $\Delta = 0.5\text{km}$ . Fig.4 shows the beam patterns of MNW and LPBM.

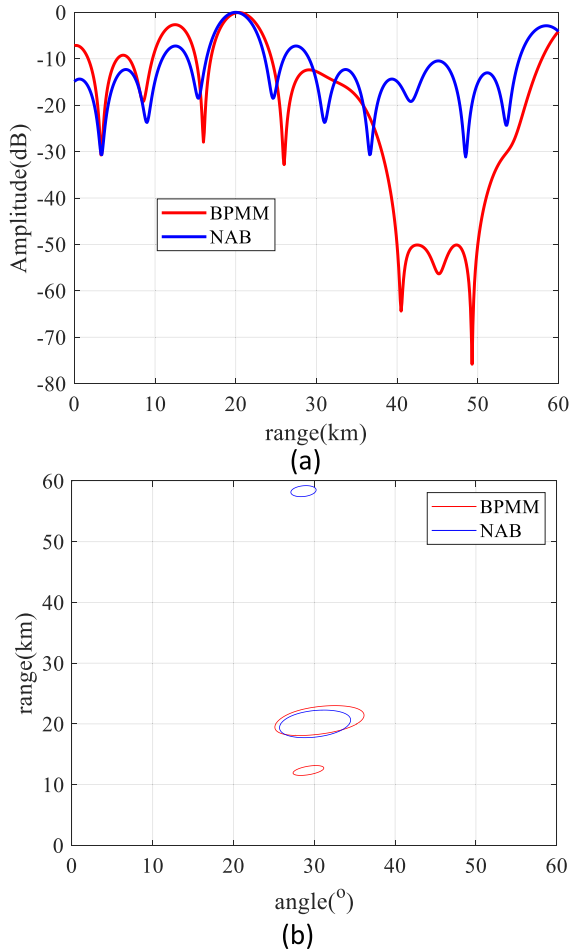


FIGURE 2. Comparative results of (a) the gain in the range dimension and (b) the spatial energy focusing.

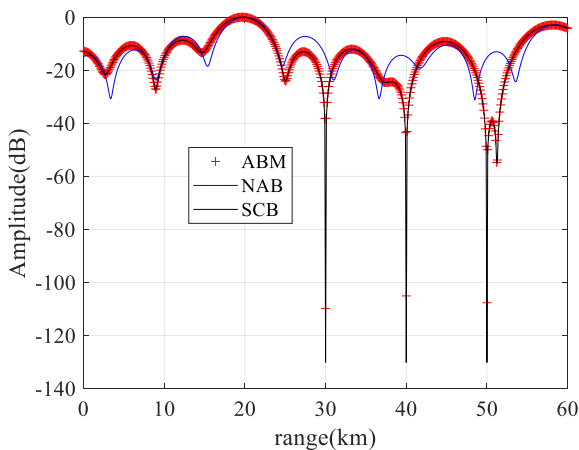


FIGURE 3. Comparative results of beam pattern in the range dimension.

As we can see in Fig.4, both MNW and LPBM can achieve robust suppression of interference by implementing null widening at the interference. The beam pattern of MNW has multiple maximum points near the target, which is not conducive to the detection of the target, while LPBM

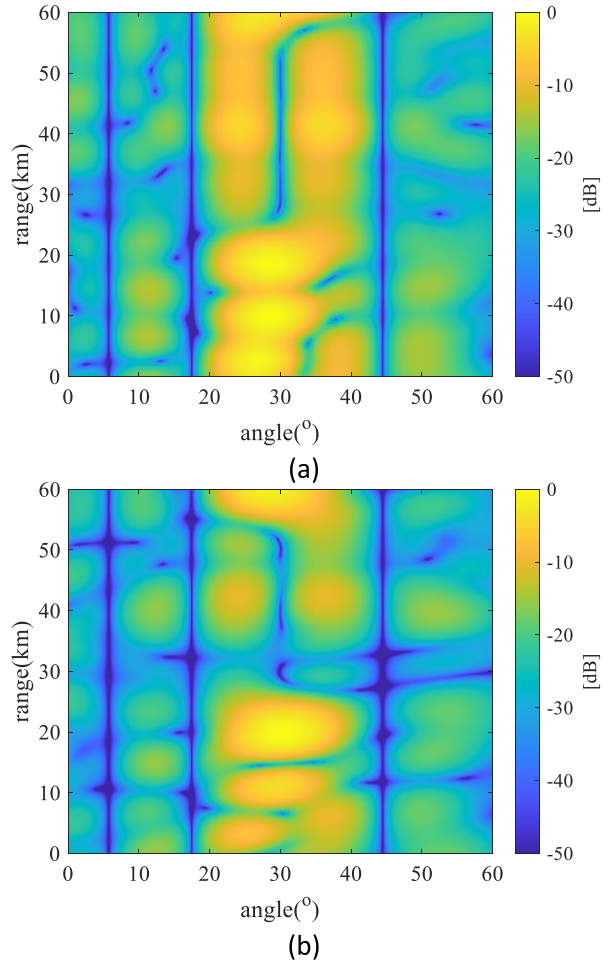


FIGURE 4. The beam patterns of (a) MNW and (b) LPBM.

effectively avoids this problem. The comparative results of beam pattern in the range dimension are shown in Fig.5.

We can observe from Fig.5 that SCB has a good interference suppression performance, but it is sensitive to steering vectors and has poor robustness. MNW and LPBM have good robust interference suppression capability. Then, we simulate and compare the robustness of each method. Suppose the actual coordinates of the three interference sources are (30.5km, 30°), (40.5km, 30°), and (50.5km, 30°). Fig.6 shows the change process of the output signal-to-interference-plus-noise (SINR) value of each method with the change of the input SNR value.

We can see from Fig.6 that Both MNW and LBPM can effectively suppress interference and improve the output SINR. With the increase of SNR, the output SINR of each method tends to be stable because the influence of noise on the signal becomes weaker at this time. Although the SNR of the output SINR of the MNW is larger than the output SINR of the LPBM, The beam gain of MNW has multiple maximum values and is not at the target, which is not conducive to the positioning of the target.

Finally, we test the robustness of each method by comparing the accuracy of the target power estimates.

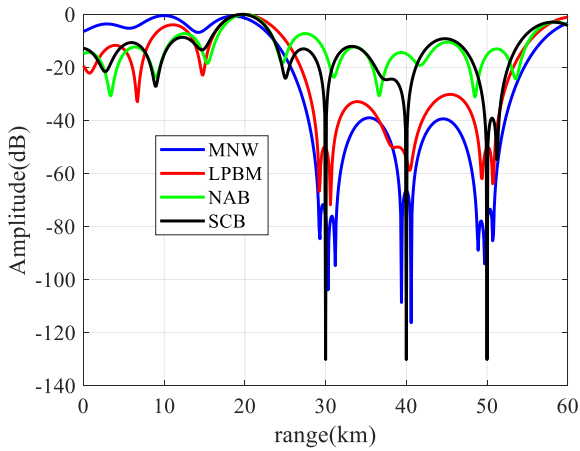


FIGURE 5. Range-dimensional beam comparison results.

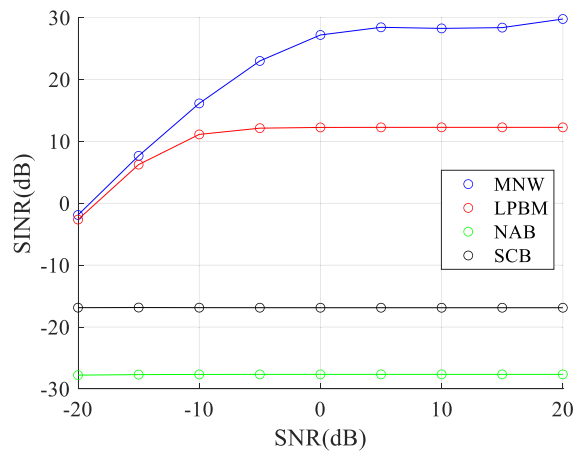


FIGURE 6. Output SINR comparison.

After removing the array aperture gain factor, the target power estimation formula can be rewritten as:

$$\rho = (\|\mathbf{W}^H \mathbf{y}(r, \theta)\| / N_t N_r)^2 \quad (28)$$

We assume that six signal-dependent interferers are at the same angle as the target. The ranges obtained from the prior information are 30km, 35km, 40km, 45km, 50km, and 55km, and the actual ranges are 30.5km, 35.5km, 40.5km, 45.5km, 50.5km, and 55.5km. Let the noise power be 0dB, then the target power is 20dB, and the interference power is 40dB. The number of interferences is increased successively, and the result of power estimation is shown in Fig.6.

We can observe from Fig.7 that the robustness of SCB and NAB is not good, while the robustness of MNW and LPBM is better. On the one hand, the target power obtained by MNW is smaller than the actual value because the target is located near the maximum value. On the other hand, LPBM is not sensitive to the variation of interference power, and its ability to suppress interference depends on a pre-set threshold. The interference location is the same as example 2. The power of six interferers is changed, and the result of estimating the target power is shown in Fig. 8.

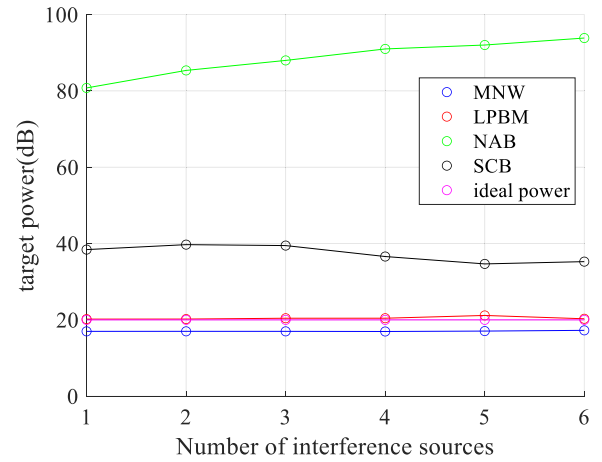


FIGURE 7. Target power estimation comparison.

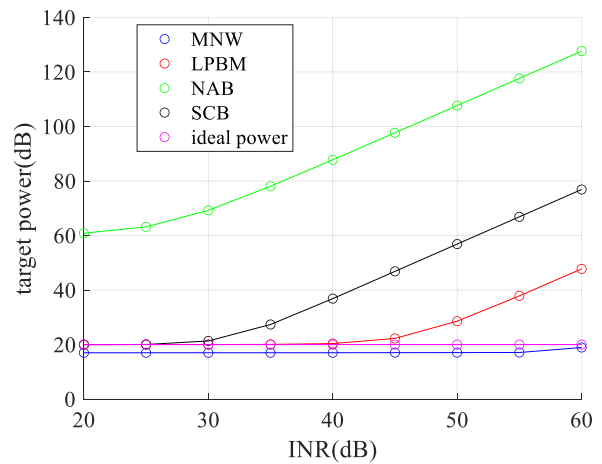


FIGURE 8. Target power estimation under different INR.

It is noted from Fig.8 that when the INR is greater than 50dB, the LPBM method also begins to have obvious estimation errors because we set the threshold to  $\tau = -50dB$  in LPBM. However, MNW has always maintained a good power estimation performance. Therefore, using the MNW results in a more accurate estimate of the target power when the interference power is unknown. Conversely, using LPBM results in a more accurate target power estimate because we can change the threshold  $\tau$  at this point.

## VI. CONCLUSION

This paper mainly studies the problem of suppressing main-lobe interference by applying robust adaptive beamforming for the matrix method. We first solve the four schemes of the design by establishing SDP problems and then verify the robustness by estimating the target signal power. It is worth pointing out that we obtain the weighting matrix by the singular value decomposition method, which brings two advantages: improving the robustness and avoiding the non-convexity problem of rank-one constraint by applying matrix weighting. The performance achieved by the proposed MNW and LPBM methods is satisfactory and can achieve interference suppression.

## ACKNOWLEDGMENT

The authors would like to thank the anonymous reviewers for their valuable comments and suggestions to improve the readability of this paper.

## REFERENCES

- [1] M. Zhang, X. Zhang, W. Song, W. Kong, and Z. Zhang, "Mixed jamming suppression algorithm for phased array radar," *J. Eng.*, vol. 2019, no. 20, pp. 7179–7184, Oct. 2019.
- [2] F. Wang, V. Balakrishnan, P. Y. Zhou, J. J. Chen, R. Yang, and C. Frank, "Optimal array pattern synthesis using semidefinite programming," *IEEE Trans. Signal Process.*, vol. 51, no. 5, pp. 1172–1183, May 2003.
- [3] P. Kassakian, "Magnitude least-squares fitting via semidefinite programming with applications to beamforming and multidimensional filter design," in *Proc. IEEE Int. Conf. Acoust., Speech, Signal Process.*, Mar. 2005, pp. 18–23.
- [4] X. Zheng, P. Stoica, J. Li, and R. Wu, "Adaptive arrays for broadband communications in the presence of co-channel interference," in *Proc. 40th Asilomar Conf. Signals, Syst. Comput.*, 2006, pp. 1032–1036.
- [5] J. Capon, "High resolution frequency-wavenumber spectrum analysis," *Proc. IEEE*, vol. 57, no. 8, pp. 1408–1418, Aug. 1969.
- [6] J. Li, Y. Xie, P. Stoica, X. Zheng, and J. Ward, "Beampattern synthesis via a matrix approach for signal power estimation," *IEEE Trans. Signal Process.*, vol. 55, no. 12, pp. 5643–5657, Dec. 2007.
- [7] L. Tao et al., "Robust beamforming via Matrix weighted method," *Chin. J. Radio Sci.*, vol. 29, no. 1, pp. 135–142, 2014.
- [8] P. Antonik, M. C. Wicks, H. D. Griffiths, and C. J. Baker, "Frequency diverse array radars," *Proc. IEEE Radar Conf.*, Verona, Italy, Apr. 2006, pp. 215–217.
- [9] M. Secmen, S. Demir, A. Hizal, and T. Eker, "Frequency diverse array antenna with periodic time modulated pattern in range and angle," in *Proc. IEEE Radar Conf.*, Boston, MA, USA, Apr. 2007, pp. 427–430.
- [10] Y. Xu, X. Shi, W. Li, J. Xu, and L. Huang, "Low-sidelobe range-angle beamforming with FDA using multiple parameter optimization," *IEEE Trans. Aerosp. Electron. Syst.*, vol. 55, no. 5, pp. 2214–2225, Oct. 2019.
- [11] A. Basit, W. Khan, S. Khan, and I. M. Qureshi, "Development of frequency diverse array radar technology: A review," *IET Radar, Sonar Navigat.*, vol. 12, no. 2, pp. 165–175, Feb. 2018.
- [12] P. Antonik, "An investigation of a frequency diverse array," Ph.D. dissertation, Univ. College London, London, U.K., 2009.
- [13] M. Tan, C. Wang, and Z. Li, "Correction analysis of frequency diverse array radar about time," *IEEE Trans. Antennas Propag.*, vol. 69, no. 2, pp. 834–847, Feb. 2021.
- [14] P. F. Sannmartino, C. J. Baker, and H. D. Griffiths, "Frequency diverse MIMO techniques for radar," *IEEE Trans. Aerosp. Electron. Syst.*, vol. 49, no. 1, pp. 201–222, Jan. 2013.
- [15] W. Khan, I. M. Qureshi, and S. Saeed, "Frequency diverse array radar with logarithmically increasing frequency offset," *IEEE Antennas Wireless Propag. Lett.*, vol. 14, pp. 499–502, 2015.
- [16] Y. Wang, G. Huang, and W. Li, "Transmit beampattern design in range and angle domains for MIMO frequency diverse array radar," *IEEE Antennas Wireless Propag. Lett.*, vol. 16, pp. 1003–1006, 2016.
- [17] A. Basit, I. M. Qureshi, W. Khan, S. U. Rehman, and M. M. Khan, "Beam pattern synthesis for an FDA radar with Hamming window-based nonuniform frequency offset," *IEEE Antennas Wireless Propag. Lett.*, vol. 16, pp. 2283–2286, 2017.
- [18] Y. Ma, P. Wei, and H. Zhang, "General focusing beamformer for FDA: Mathematical model and resolution analysis," *IEEE Trans. Antennas Propag.*, vol. 67, no. 5, pp. 3089–3100, May 2019.
- [19] J. Xiong, W.-Q. Wang, H. Shao, and H. Chen, "Frequency diverse array transmit beampattern optimization with genetic algorithm," *IEEE Antennas Wireless Propag. Lett.*, vol. 16, pp. 469–472, Jun. 2016.
- [20] Y. Liao, J. Wang, and Q. H. Liu, "Transmit beampattern synthesis for frequency diverse array with particle swarm frequency offset optimization," *IEEE Trans. Antennas Propag.*, vol. 69, no. 2, pp. 892–901, Feb. 2021.
- [21] Y. Xu, X. Shi, W. Li, and J. Xu, "Flat-top beampattern synthesis in range and angle domains for frequency diverse array via second-order cone programming," *IEEE Antennas Wireless Propag. Lett.*, vol. 15, pp. 1479–1482, 2016.
- [22] H. Shao, J. Dai, J. Xiong, H. Chen, and W.-Q. Wang, "Dot-shaped range-angle beampattern synthesis for frequency diverse array," *IEEE Antennas Wireless Propag. Lett.*, vol. 15, pp. 1703–1706, 2016.
- [23] Q. Li, L. Huang, H. C. So, H. Xue, and P. Zhang, "Beampattern synthesis for frequency diverse array via reweighted  $\ell_1$  iterative phase compensation," *IEEE Trans. Aerosp. Electron. Syst.*, vol. 54, no. 1, pp. 467–475, Feb. 2018.
- [24] Z. Ding and J. Xie, "Joint transmit and receive beamforming for cognitive FDA-MIMO radar with moving target," *IEEE Sensors J.*, vol. 21, no. 18, pp. 20878–20885, Sep. 2021.
- [25] L. Lan, G. Liao, J. Xu, Y. Zhang, and B. Liao, "Transceive beamforming with accurate nulling in FDA-MIMO radar for imaging," *IEEE Trans. Geosci. Remote Sens.*, vol. 58, no. 6, pp. 4145–4159, Jun. 2020.
- [26] P. Gong, W.-Q. Wang, F. Li, and H. C. So, "Sparsity-aware transmit beamspace design for FDA-MIMO radar," *Signal Process.*, vol. 144, pp. 99–103, Mar. 2018.
- [27] J. Xu, J. Kang, G. Liao, and H. C. So, "Mainlobe deceptive jammer suppression with FDA-MIMO radar," in *Proc. IEEE 10th Sensor Array Multichannel Signal Process. Workshop (SAM)*, Jul. 2018, pp. 504–508.
- [28] L. Lan, G. Liao, J. Xu, Y. Zhang, and F. Fioranelli, "Suppression approach to main-beam deceptive jamming in FDA-MIMO radar using nonhomogeneous sample detection," *IEEE Access*, vol. 6, pp. 34582–34597, 2018.
- [29] Z.-Q. Luo, W.-K. Ma, A. M.-C. So, Y. Ye, and S. Zhang, "Semidefinite relaxation of quadratic optimization problems," *IEEE Signal Process. Mag.*, vol. 27, no. 3, pp. 20–34, May 2010.
- [30] M. Grant and S. Boyd. (Mar. 2014). *CVX: MATLAB Software for Disciplined Convex Programming, Version 2.1*. [Online]. Available: <http://cvxr.com/cvx>
- [31] X. Zhang, Z. He, X. Zhang, and W. Peng, "High-performance beampattern synthesis via linear fractional semidefinite relaxation and quasi-convex optimization," *IEEE Trans. Antennas Propag.*, vol. 66, no. 7, pp. 3421–3431, Jul. 2018.

• • •